



Original article

Design, synthesis and biological evaluation of thiazole- and indole-based derivatives for the treatment of type II diabetes

Qinyuan Xu, Li Huang, Juan Liu, Liang Ma, Tao Chen, Jinying Chen, Fei Peng, Dong Cao, Zhuang Yang, Neng Qiu, Jingxiang Qiu, Guangcheng Wang, Xiaolin Liang, Aihua Peng, Mingli Xiang, Yuquan Wei, Lijuan Chen*

State Key Laboratory of Biotherapy, West China Hospital, West China Medical School, Sichuan University, Keyuan Road 4, Gaopeng Street, Chengdu 610041, China

ARTICLE INFO

Article history:

Received 25 November 2011
Received in revised form
29 February 2012
Accepted 2 March 2012
Available online 13 March 2012

Keywords:

Ap2
Thiazole- and indole-based
TNF- α
Diet-induced obesity

ABSTRACT

Present studies have shown that the lipid carrier has a significant role in several aspects of metabolic syndrome in A-FABP/ap2-deficient mice, including type 2 diabetes and atherosclerosis. 38 Thiazole- and indole-based derivatives were synthesized and investigated for their inhibitory effects on the production of LPS-stimulated TNF- α . Among them, **12b** exhibited an excellent inhibitory efficiency compared to **BMS309403** (95% vs. 85%) at the concentration of 10 μ M and a binding affinity for ap2 with the apparent K_i values 33 nM. Oral administration of **12b** at a dosage of 50 mg/kg effectively reduced the levels of plasma blood glucose, triglycerides, insulin, total cholesterol and alanine aminotransferase in high-fat/diet-induced obesity model. The results highlighted that **12b** was a potent anti-diabetic agent.

© 2012 Elsevier Masson SAS. All rights reserved.

1. Introduction

Type II diabetes (T2D) is the most common disorder of metabolic homeostasis characterized by insulin resistance and dyslipidemia, accounting for 90–95% of all cases of diabetes. In 2010, approximately 285 million people suffer from diabetes, corresponding to 6.4% of the world's population, and the figure is predicted to increase to 438 million by 2030. Insulin resistance and dyslipidemia are closely associated with catabolic or lipodystrophic conditions and with pathological states of over-nutrition (e.g., obesity-related diabetes). The main feature of these metabolic disorders is the abnormal elevation of serum levels of pro-inflammatory cytokines such as tumor necrosis factor- α (TNF- α), interleukin-1 β (IL-1 β), and IL-6, etc. [1,2]. TNF- α protein is secreted by activated monocyte/macrophage and highly expressed in adipose tissue of obese animal and human with T2D [3,4]. Specifically, it has been reported that obese mice with the lack of either TNF- α production or TNF- α receptor could be protected against the development of insulin resistance [5,6]. Therefore, blockage of the over-expression of TNF- α might be an effective strategy for the prevention and treatment of T2D [7].

Considerable studies have focused on the drug target of T2D, including glucagon-like Peptide-1 (GLP-1), dipeptidyl peptidase-4 (DPP-4), peroxisome proliferators activated receptor γ (PPAR γ), protein tyrosine phosphatase 1B (PTP1B) etc. Recently, adipocyte fatty acid binding protein (A-FABP or ap2), a 14.6 kDa cytosolic protein that bind with high affinity to saturated and unsaturated long-chain fatty acids, has become a pivotal target with more attention. Ap2 is highly expressed in adipocytes and macrophages, and could be regulated by PPAR γ agonists, insulin, and fatty acids. Ap2 played significant roles in many aspects of metabolic syndrome (e.g., glucose and lipid homeostasis), and the over-expression of ap2 invariably occurred to obese mice or human. The ap2-deficient mice access to a high-fat diet were protected against glucose tolerance and insulin resistance in contrast to the wild type ones [8]. Furthermore, the production of TNF- α in response to lipopolysaccharide (LPS) was down-regulated in ap2 knockout mice [9].

Up to date, several potent small-molecule inhibitors of ap2 such as **BMS309403**, **HTS01037**, and **1** have been rationally designed and developed for the treatment of T2D (Fig. 1) [10–12]. Inspection of their structural features highlighted that the five-membered heterocyclic ring and carboxylic group seemed to be crucial for anti-ap2 potency. Furthermore, there were also literature reported that some compounds with indole had anti-inflammatory activity [13,14]. Thus, the results encouraged us to develop more potent drug-like candidates.

* Corresponding author. Tel.: +86 28 85164063; fax: +86 28 85164060.
E-mail address: lijuan17@hotmail.com (L. Chen).

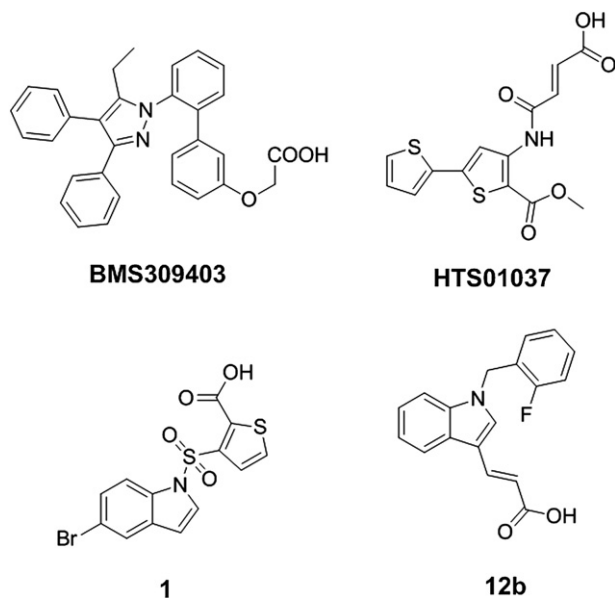


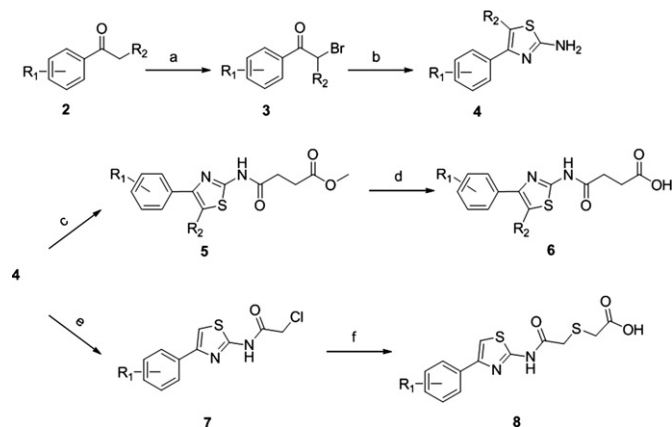
Fig. 1. Structure of BMS309403, HTS01037, 1 and 12b.

In this study, a series of thiazole- and indole-based derivatives has been synthesized and their inhibitory effects on the production of TNF- α were subsequently performed in LPS-induced RAW 264.7 cells. At a concentration of 10 μ M, (*E*)-3-(1-(2-fluorobenzyl)-1*H*-indol-3-yl)acrylic acid (**12b**) was found to possess an excellent inhibitory rate against the production of TNF- α in contrast to BMS309403 (95% vs. 85%), leading to the establishment of a SAR. **12b** was also evidenced as a potent α 2 inhibitor with the apparent K_i value of 33 nM by a fluorescent 1,8-anilino-8-naphthalene sulfonate (ANS) assay. Importantly, oral administration of **12b** at a dosage of 50 mg/kg improved the weight gain and serum levels of blood glucose, TG, insulin, total cholesterol and ALT in diet-induced obesity HF, highlighting that **12b** was an orally active anti-diabetic candidate.

2. Chemistry

The thiazole analogues **6a–m** and **8a–d** were prepared starting from the reaction of various acetophenones **2** and copper (II) bromide to give **3** (Scheme 1) [15]. The α -bromoketones **3** were then reacted with thioureas to give the corresponding thiazoles **4** via cyclization reactions. To prepare the final products **6** and **8**, intermediates **4** were divided into two routes as shown in Scheme 1. When treated with 4-methoxy-4-oxobutanoic acid in the presence of DMAP and EDCI, yielded **5**, and then the hydrolysis of **5** with sodium hydroxide provided corresponding carboxylic acids **6**. When treated with chloroacetyl chloride catalyzed by Et₃N, provided **7**, and then reacted with 2-mercaptoacetic acid in anhydrous THF to yielded **8**.

The indole analogues **12a–k**, **16a–g** and **18a–e** were outlined in Schemes 2–4. The coupling of *N*-unsubstituted 1*H*-indole-3-carbaldehydes **9** with benzyl bromides **10**, using potassium hydroxide as base, converted to intermediates **11**. The synthesis of the final products **12** were carried out by adding malonic acid to a solution of **11** dissolved in pyridine in the presence of piperidine catalyst (Scheme 2). In theory, *E* and *Z* geometrical isomers around the exocyclic double bond (CH=C) are possible for 3-(1-benzyl-1*H*-indol-3-yl)acrylic acid derivatives. However, on the basis of literature data for similar compounds, these compounds belong to the *E*-configuration [16]. The *E*-configuration of similar compounds also



Scheme 1. General synthesis of thiazole-based derivatives. Reagents and conditions: (a) CuBr₂, EtOAc-CHCl₃; (b) thiourea, EtOH; (c) 4-methoxy-4-oxobutanoic acid, DMAP, EDCI, room temperature; (d) NaOH, HCl; (e) 2-chloroacetyl chloride, Et₃N; (f) 2-mercaptoacetic acid, Et₃N.

has been identified from ¹H NMR spectra. The coupling constants (*J*) of these compounds were all between 15.6 and 16.4 Hz in the range from 6.25 to 6.48 ppm in dimethylsulfoxide (DMSO)-*d*₆ solution, while the values of the *Z*-isomer were commonly between 7 and 12 ppm.

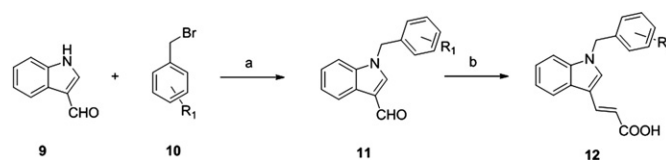
The formyl group was added at C₃ of **13** by the Vielsmeier reaction utilizing POCl₃ and DMF (Scheme 3) [17]. A similar sequence of reactions was carried out to prepare the intermediates **15** and final products **16**, starting from the appropriately substituted derivatives. Benzoylation of the amide **17** was achieved by deprotonation of the amide with sodium hydride and then reacted with the benzoylation agent (Scheme 4).

3. Results and discussion

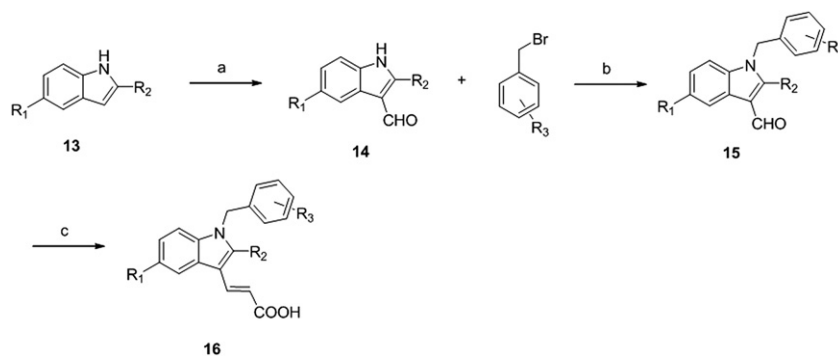
3.1. Inhibition of LPS-induced TNF- α production in RAW 264.7 cells

All synthesized compounds were evaluated for their ability to inhibit the production of LPS-induced TNF- α in RAW 264.7 cells. The inhibitory rate was depicted in Table 1. BMS309403 was used as positive control. In the series of thiazole-based compounds, we started from halogen substitution on the phenyl ring. We can find the compounds with a *para*-substitution demonstrated moderate inhibitory potency (e.g., **6a**, **6e** and **6k**), while compound **6b** and **6f** that contained *ortho* or *meta* substitutions showed poor inhibitory effect. It is interesting to note that the 3,4-difluoro analogue **6g** showed more potent inhibitory activity as compared to the 3,4-dichloride **6f**. It is surprising that methyl substitution on the *para* position of the phenyl ring showed good activity, while methoxyl didn't work. The introduction of mercaptoacetic acid to the side did not result in increased activity (see **8a–d**).

As shown in Table 1, introduction of phenyl ring which contained various substitutions replaced the hydrogen on the nitrogen. Based on our previous SAR of the thiazole-based compounds, they



Scheme 2. General synthesis of **12a–k**. Reagents and conditions: (a) KOH, EtOH, acetone; (b) malonic acid, pyridine, piperidine, 100 °C.

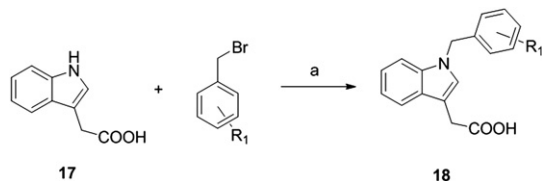


Scheme 3. General synthesis of **16a–g**. Reagents and conditions: (a) POCl₃, DMF, NaOH; (b) KOH, EtOH, acetone; (c) malonic acid, pyridine, piperidine, 100 °C.

had a similar law that the compounds which had *ortho*- or *para*-substitutions on the phenyl ring showed good activity (e.g., **12b**, **12e**, **12f** and **12k**), while the *meta* ones had a little or no activity (e.g., **12c**, **16d**, **16e**, **16g** and **18d**). We also observed that the compounds which had strongly electron-withdrawing groups only showed moderate inhibitory activity (e.g., **12h** and **12i**). Further, the 5-substituted indole analogues (e.g., **16a**, **16b**, **16d–f**) were synthesized. As the results, the methoxyl substituted had higher inhibition rate (e.g., **16b** and **16f**) while the methyl was poor (**16a**). However, compound had methyl at the 2-position (**16c**) indicated good effect. More important, fluorine played a crucial role to the inhibitors of TNF- α . Almost all the compounds which had *ortho*- or *para*- fluorine showed excellent activity (see **12b**, **12k**, **16b**, **16c**, **16f** and **18e**). The indole acetic acid analogues (see **18a–e**) were also evaluated *in vitro*, there were the similar SAR as discussed above.

3.2. K_i values and docking study of **12b**

The compound **12b** was selected for further study because of its strongest inhibitory activity among these derivatives. In a fluorescent 1,8-anilino-8-naphthalene sulphonate (ANS) binding displacement assay, **12b** exhibited similar K_i values to **BMS309403** for mouse ap2 (33 nM vs. 29 nM). Meanwhile, we docked the **12b** to the protein of ap2 (Fig. 2). The X-ray crystal structure of fatty acid-binding protein 4 (A-FABP) was obtained from protein data bank (PDB ID: 2QM9) with 2.31 Å resolution. Ligand molecules drawn with ChemBio3D were docked to the binding site of A-FABP by the aid of a protein-ligand docking program FRED 2.2.5 (OpenEye Scientific Software, Santa Fe, NM 87508) [18,19]. The binding site of the protein was prepared by employing FRED RECEPTOR 2.2.5 (OpenEye Scientific Software, Santa Fe, NM 87508). AM1-BCC partial charges were assigned to ligand molecules while Merck Molecular Mechanics Force Field (MMFF) partial charges were assigned to protein [20–22]. In the figure, we can find that **12b** formed hydrogen bonds to Tyr 19 and Arg 78. The π -cation interaction between the indole moiety of the compound and the side chain of Arg 126 is shown with orange mark.



Scheme 4. General synthesis of **18a–e**. Reagents and conditions: (a) NaH, DMF.

3.3. *In vivo* activity in diet-induced obesity (DIO) rats

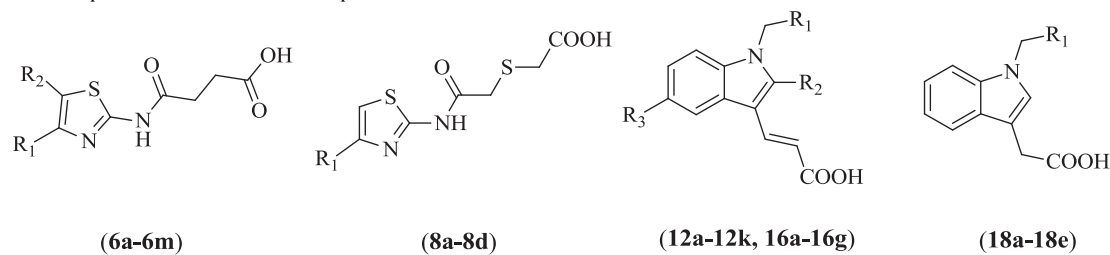
For further investigate *in vivo* studies of compound **12b**, we established a high-fat/diet-induced obesity (DIO) rat model. Male C57BL/6J rats (age range: 7–8 weeks) were purchased from Western China Experimental Animal Center. To get a fully developed insulin-resistant diet-induced obese (DIO) animal phenotype, the animals were fed with a normal diet or a high-fat diet (kcal: 60% of energy derived from fat, 20% from protein and 20% from carbohydrates, D12494 Research Diet, USA) for 8 weeks. Then, the rats which were fed with a high-fat diet were divided into two groups fed with the high-fat diet as before (HF) or with the same food and oral administration of **12b** once a day at a dose of 50 mg/kg. The body weight of the two groups were respectively from 22.42 \pm 0.72 g and 24.08 \pm 0.61 g at the beginning to 32.26 \pm 4.71 g and 29.18 \pm 2.54 g after 8 weeks. The weight gain rate of **12b**-treated was 21.18% compared with HF groups 43.89% (Fig. 3A and B). While there was no significant difference in food intake between HF and treated groups (Fig. 4). In contrast, blood glucose levels had obviously decreased after treatment with **12b** (Fig. 5A). Throughout the *in vivo* experiment, decrements in levels of triglyceride (TG), total cholesterol (TC), alanine aminotransferase (ALT) were 27.13%, 38.52% and 26.66% respectively (Fig. 5B, C and D).

Meanwhile, glucose tolerance tests revealed a significant improvement in glucose metabolism in the **12b**-treated group (Fig. 6A). Similarly, insulin tolerance tests showed significantly increased insulin sensitivity in the DIO rats treated with **12b** (Fig. 6B). To evaluate whether **12b** improved fat deposition in C57BL/6J rat HF with diet-induced obesity, liver tissues from HF and **12b**-treated rats were processed for H&E staining assay (Fig. 7). We can find many fat balloons in the liver tissue of the HF group (Fig. 7A), while the fat droplets significantly decreased after **12b**-treated as evidenced by H&E staining. In general, **12b** demonstrated an excellent effect for the treatment of diabetes and obesity.

4. Conclusion

We performed the synthesis and SAR of thiazole-based and indo-based compounds. Several exhibited significantly inhibitory effect in LPS-induced TNF- α production. The most effective compound **12b** was also a high affinity ligand of A-FABP/ap2 with apparent K_i values 33 nM. In the diet-induced obesity (DIO) rodent model, **12b** not only control effectively the growth of the rat's weight which were fed high-fat diet, but also obviously decreased the serum levels of GLU, TC, TG, ALT. In glucose and insulin tolerance tests, it also improved glucose metabolism and increased insulin sensitivity. In general, it was worth for further investigation as a drug for treatment of diabetes.

Table 1
Inhibitory effects of all compounds on LPS-induced TNF- α production.



Compd	R ₁	R ₂	R ₃	Inhibition % ^a
6a		H		41.22
6b		H		8.56
6c		H		36.67
6d		H		12.15
6e		H		27.24
6f		H		12.38
6g		H		92.45
6h		H		NI
6i		H		35.15
6j		-CH ₃		25.23
6k		-CH ₃		27.14
6l		H		58.75

(continued on next page)

Table 1 (continued)

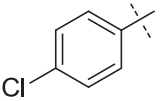
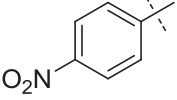
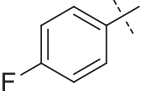
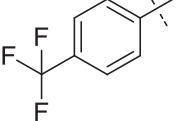
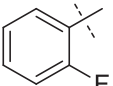
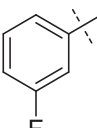
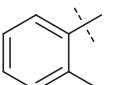
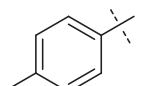
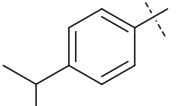
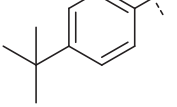
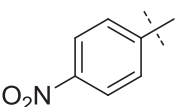
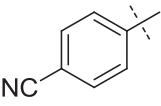
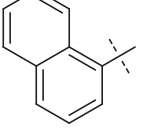
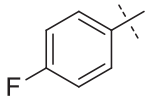
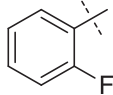
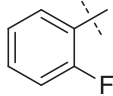
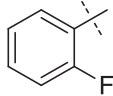
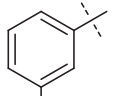
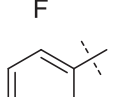
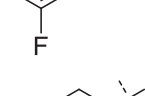
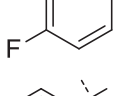
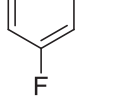
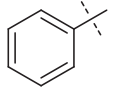
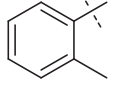
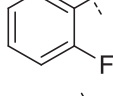
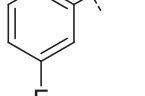
Compd	R ₁	R ₂	R ₃	Inhibition % ^a
8a				23.45
8b				43.24
8c				18.19
8d				37.26
12a		H	H	18.17
12b		H	H	95.47
12c		H	H	36.36
12d		H	H	NI
12e		H	H	66.56
12f		H	H	92.24
12g		H	H	50.18
12h		H	H	32.34
12i		H	H	31.46
12j		H	H	93.28

Table 1 (continued)

Compd	R ₁	R ₂	R ₃	Inhibition % ^a
12k		H	H	86.78
16a		H	-CH ₃	11.18
16b		H	-OCH ₃	86.67
16c		-CH ₃	H	93.27
16d		H	-CH ₃	NI
16e		H	-OCH ₃	NI
16f		H	-OCH ₃	94.28
16g		-CH ₃	H	NI
18a				52.17
18b				14.29
18c				24.72
18d				NI
18e				92.24
BMS309403				85.13

^a Values are expressed as the concentration of TNF- α in the medium of the compounds dosing group divided by it of the LPS-induced group. The concentration of all compounds are 10 μ mol/mL (NI = not inhibition).

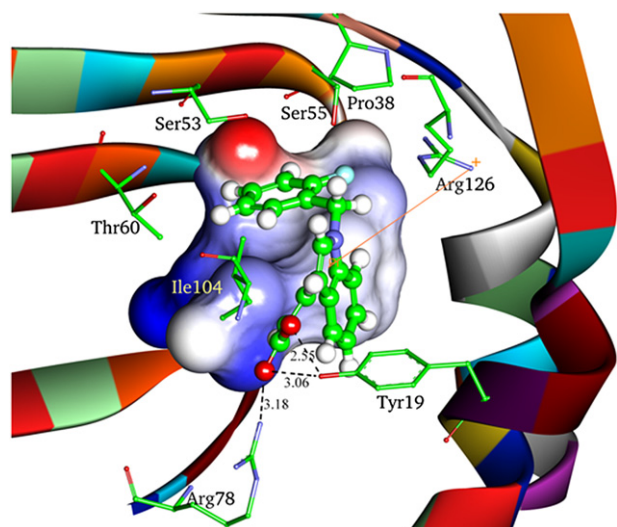


Fig. 2. The interaction mode of compound **12b** within the binding site of FABP4 (PDB ID: 2QM9).

5. Experimentals

5.1. Chemistry

Purchased reagents and anhydrous solvents were used as received. NMRs were obtained with a Bruker 400 MHz in the indicated solvent with chemical shifts (δ) reported in ppm vs. tetramethylsilane and coupling constants (J) in Hz. The multiplicity of the signal is indicated as s, singlet; d, doublet; t, triplet; q, quartet; m, multiplet, defined as all multiplet signals where overlap or complex coupling of signals makes definitive descriptions of peaks difficult. Mass Spectra (MS) were measured by Q-TOF Premier mass spectrometer utilizing electrospray ionization (ESI) (Micromass, Manchester, UK). Room temperature (RT) is within the range 20–25 °C.

5.1.1. General procedure for the synthesis of 2-bromo-1-(2-chlorophenyl)ethanone

A solution of 1-(2-chlorophenyl)ethanone (**2b**) (0.84 mL, 6.5 mmol) in anhydrous ethyl acetate (25 mL) and chloroform (25 mL) was treated with copper (II) bromide (4.33 g, 19.5 mmol) and ethanol (6 mL), stirred at 65 °C for 0.5 h. The reaction was extracted with chloroform (40 mL). The organic extracts were washed with water (3 × 30 mL), dried (Na₂SO₄), filtered, and concentrated in vacuo to give a colourless oil. ¹H NMR (CDCl₃, 400 MHz): δ 4.53 (s, 2H), 7.36–7.41 (m, 1H), 7.44–7.46 (m, 2H), 7.56 (d, 1H, J = 8.0 Hz).

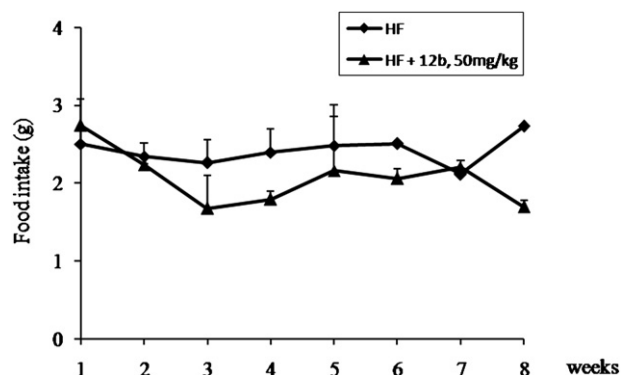


Fig. 4. The food intake in C57BL/6J rats treated with vehicle (HF) or **12b** at the state of feeding with high-fat diet for 8 weeks. The arrow bars were determined by Excel.

5.1.2. General procedure for the synthesis of 4-(2-chlorophenyl)thiazol-2-amine

The crude 2-bromo-1-(2-chlorophenyl) ethanone (0.64 mL, 4.28 mmol) was dissolved in anhydrous ethanol (10 mL) and treated with thiourea (344 mg, 4.51 mmol). After heating at reflux for 2 h, the reaction mixture was cooled to room temperature, with a yellow precipitation. The solid obtained was filtered, washed with water and ethanol and vacuum dried to afford **4b** as a yellow solid (884 mg, 98.0%). ¹H NMR (CDCl₃, 400 MHz): δ 7.12 (s, 1H), 7.46–7.55 (m, 2H), 7.62 (s, 1H), 7.63 (d, 1H, J = 1.2 Hz), 8.94 (s, 1H), 9.15 (s, 1H).

5.1.3. General procedure for the synthesis of methyl 4-(4-(2-chlorophenyl)thiazol-2-ylamino)-4-oxobutanoate

A mixture of 4-(2-chlorophenyl)thiazol-2-amine (500 mg, 2.37 mmol), DMAP (13.27 mg, 0.12 mmol), EDCI (682.43 mg, 3.55 mmol) and 4-methoxy-4-oxobutanoic acid (470.3 mg, 3.55 mmol) in chloroform (20 mL) was stirred at room temperature for 24 h. The solution was filtered, and filtrate was washed with water. The organic phase was dried (Na₂SO₄) and evaporated to dryness. The residue was purified by flash chromatography over silica gel eluting with CH₂Cl₂:EtOAc (80:1) yielded 280 mg (36.3% yield) to **5b**.

5.1.4. General procedure for the synthesis of 4-(4-(2-chlorophenyl)thiazol-2-ylamino)-4-oxobutanoic acid

A mixture of methyl 4-(4-(2-chlorophenyl)thiazol-2-ylamino)-4-oxobutanoate (100 mg, 0.31 mmol) and NaOH (123 mg, 3.1 mmol) in 1,4-dioxane (6 mL) was stirred at 60 °C for 2.5 h. After cooling to room temperature, the mixture was added water (5 mL), acidification with 4 N HCl which resulted in the formation of a white solid. The solid was washed with water and vacuum dried

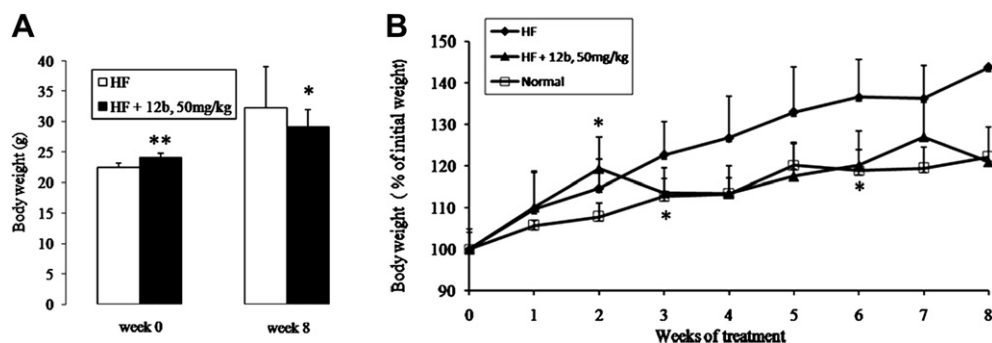


Fig. 3. Body weight and body weight gain rate of untreated and **12b**-treated DIO rat model access to HF diet. A, The body weight of treatment in C57BL/6J rats with vehicle (HF) or **12b** at the state of feeding with high-fat diet for 8 weeks. B, The body weight gain rate of feeding with high-fat diet (HF), high-fat diet added **12b** (50 mg/kg) and normal food for 8 weeks. * P < 0.05; ** P < 0.01; vs. HF group by ANOVA.

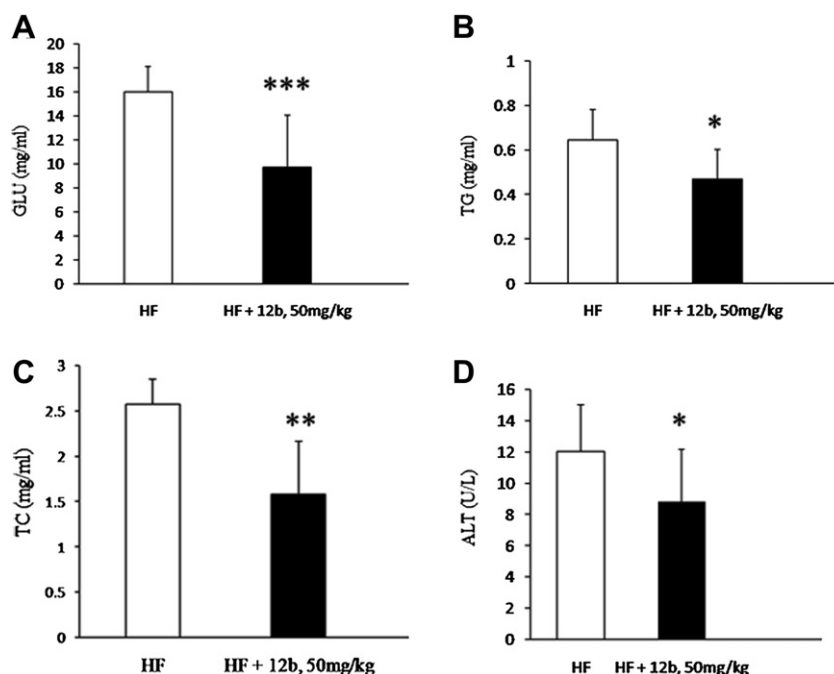


Fig. 5. Metabolic studies in **12b**-treated and untreated DIO rat model access to HF diet. A, Blood glucose levels after 8 weeks of treatment in C57BL/6J rats with vehicle (HF) or **12b** at the state of feeding with high-fat diet. B, Serum triglyceride levels after 8 weeks of treatment in C57BL/6J rats with vehicle (HF) or **12b** at the state of feeding with high-fat diet. C, Serum total cholesterol levels after 8 weeks of treatment in C57BL/6J rats with vehicle (HF) or **12b** at the state of feeding with high-fat diet. D, Serum alanine aminotransferase levels after 8 weeks of treatment in C57BL/6J rats with vehicle (HF) or **12b** at the state of feeding with high-fat diet. * $P < 0.05$; ** $P < 0.01$; *** $P < 0.001$ vs. HF group by ANOVA.

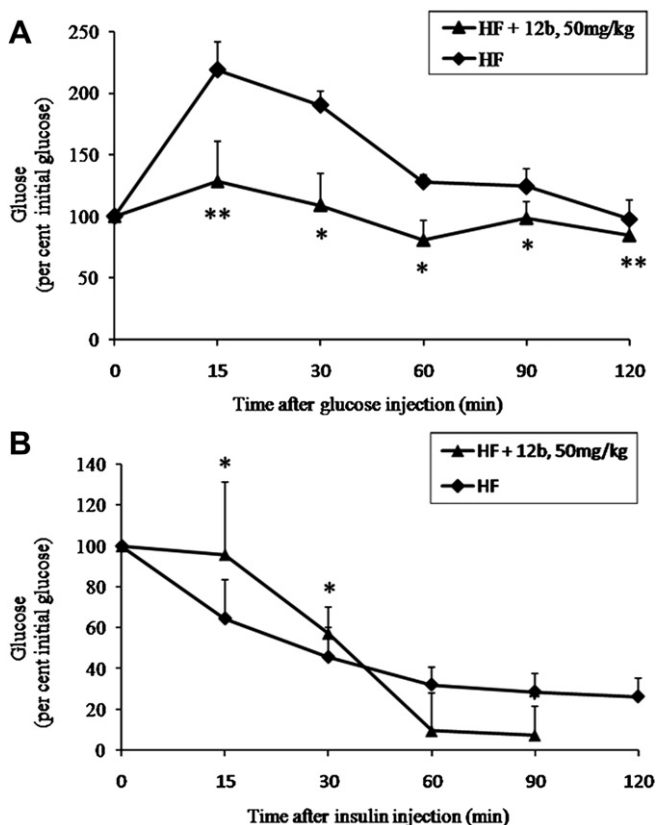


Fig. 6. Glucose and insulin tolerance tests in **12b**-treated and untreated DIO rat model access to HF diet. A, Glucose tolerance tests after 8 weeks of treatment in C57BL/6J rats with vehicle (HF) or **12b** at the state of feeding with high-fat diet. B, Insulin tolerance tests after 8 weeks of treatment in C57BL/6J rats with vehicle (HF) or **12b** at the state of feeding with high-fat diet. * $P < 0.05$ vs. HF group by ANOVA.

to afford **6b** (65.6 mg, 68.4% yield). ^1H NMR (DMSO- d_6 , 400 MHz): δ 2.57 (t, 2H, $J = 6.0$ Hz), 2.69 (t, 2H, $J = 6.0$ Hz), 7.36–7.45 (m, 2H), 7.54 (d, 1H, $J = 8.0$ Hz), 7.59 (s, 1H), 7.82 (d, 1H, $J = 7.6$ Hz), 12.23 (s, 1H), 12.33 (s, 1H); MS (ESI), m/z : 309.30 [M – H] $^-$.

5.1.4.1. 4-((4-(4-Chlorophenyl)thiazol-2-yl)amino)-4-oxobutanoic acid (**6a**). Yield 72.5%. ^1H NMR (DMSO- d_6 , 400 MHz): δ 2.57 (t, 2H, $J = 6.8$ Hz), 2.69 (t, 2H, $J = 6.8$ Hz), 6.48–7.51 (m, 2H), 7.67 (s, 1H), 7.79 (d, 1H, $J = 8.8$ Hz), 7.90 (d, 1H, $J = 8.4$ Hz), 12.32 (s, 1H); ^{13}C NMR (DMSO- d_6 , 100 MHz): δ 28.80, 30.33, 109.05, 127.82, 129.22, 132.67, 133.62, 147.95, 158.54, 171.14, 174.06; MS (ESI), m/z : 309.27 [M – H] $^-$.

5.1.4.2. 4-Oxo-4-(4-*p*-tolylthiazol-2-ylamino)butanoic acid (**6c**). Yield 62.8%. ^1H NMR (DMSO- d_6 , 400 MHz): δ 2.30 (s, 3H), 2.56 (t, 2H, $J = 6.4$ Hz), 2.68 (t, 3H, $J = 6.4$ Hz), 7.22 (d, 2H, $J = 8.0$ Hz), 7.52 (s, 1H), 7.77 (d, 2H, $J = 8.0$ Hz), 12.15 (s, 1H), 12.27 (s, 1H); MS (ESI), m/z : 289.33 [M – H] $^-$.

5.1.4.3. 4-Oxo-4-(4-(4-(trifluoromethyl)phenyl)thiazol-2-ylamino)butanoic acid (**6d**). Yield 75.2%. ^1H NMR (DMSO- d_6 , 400 MHz): δ 2.58 (t, 3H, $J = 6.4$ Hz), 2.70 (t, 3H, $J = 6.4$ Hz), 7.79 (d, 2H, $J = 8.4$ Hz), 7.85 (s, 1H), 8.10 (d, 2H, $J = 8$ Hz), 12.38 (s, 1H); MS (ESI), m/z : 343.30 [M – H] $^-$.

5.1.4.4. 4-((4-(4-Fluorophenyl)thiazol-2-yl)amino)-4-oxobutanoic acid (**6e**). Yield 82.5%. ^1H NMR (DMSO- d_6 , 400 MHz): δ 2.57 (t, 2H, $J = 6.4$ Hz), 2.69 (t, 2H, $J = 6.4$ Hz), 7.27 (t, 2H, $J = 8.8$ Hz), 7.60 (s, 1H), 7.91–7.95 (m, 2H), 12.22 (s, 1H), 12.30 (s, 1H); MS (ESI), m/z : 293.27 [M – H] $^-$.

5.1.4.5. 4-(4-(3,4-Dichlorophenyl)thiazol-2-ylamino)-4-oxobutanoic acid (**6f**). Yield 43.7%. ^1H NMR (DMSO- d_6 , 400 MHz): δ 2.57 (t, 2H, $J = 6.4$ Hz), 2.69 (t, 2H, $J = 6.4$ Hz), 7.69 (d, 1H, $J = 8.4$ Hz), 7.83 (s,

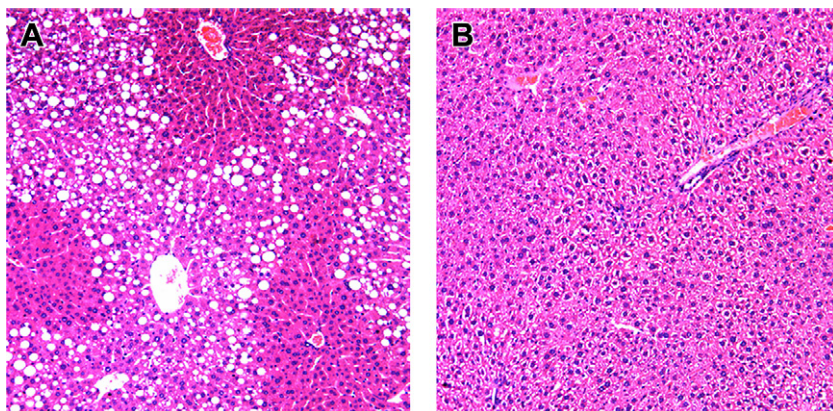


Fig. 7. H&E staining of liver sections of untreated and **12b**-treated DIO rat model access to HF diet. A, H&E staining of liver sections of untreated C57BL/6J rats access to high-fat diet. B, H&E staining of liver sections of **12b**-treated C57BL/6J rats access to high-fat diet.

1H), 7.87 (dd, 1H, $J_{1,2} = 2.0$ Hz, $J_{1,3} = 8.4$ Hz), 8.13 (d, 1H, $J = 2.0$ Hz), 12.24 (s, 1H), 12.38 (s, 1H); MS (ESI), m/z : 343.24 [M – H][–].

5.1.4.6. 4-(4-(3,4-Difluorophenyl)thiazol-2-ylamino)-4-oxobutanoic acid (**6g**). Yield 48.5%. ¹H NMR (DMSO-*d*₆, 400 MHz): δ 2.57 (t, 2H, $J = 6.4$ Hz), 2.69 (t, 2H, $J = 6.4$ Hz), 7.48 (q, 1H, $J_{1,2} = 8.4$ Hz, $J_{1,3} = 10.4$ Hz), 7.72 (s, 1H), 7.74–7.77 (m, 1H), 7.88–7.93 (m, 1H), 12.24 (s, 1H), 12.34 (s, 1H); MS (ESI), m/z : 311.26 [M – H][–].

5.1.4.7. 4-(4-(4-Methoxyphenyl)thiazol-2-ylamino)-4-oxobutanoic acid (**6h**). Yield 55.8%. ¹H NMR (DMSO-*d*₆, 400 MHz): δ 2.56 (t, 2H, $J = 6.4$ Hz), 2.68 (t, 2H, $J = 6.4$ Hz), 5.98 (d, 2H, $J = 8.4$ Hz), 7.44 (s, 1H), 7.81 (d, 2H, $J = 8.4$ Hz), 12.22 (s, 1H), 12.26 (s, 1H); MS (ESI), m/z : 305.22 [M – H][–].

5.1.4.8. 4-(4-(2,4-Dichlorophenyl)thiazol-2-ylamino)-4-oxobutanoic acid (**6i**). Yield 45.6%. ¹H NMR (DMSO-*d*₆, 400 MHz): δ 2.58 (t, 2H, $J = 6.4$ Hz), 2.70 (t, 2H, $J = 6.4$ Hz), 7.53 (dd, 1H, $J_{1,2} = 2.0$ Hz, $J_{1,3} = 8.4$ Hz), 7.66 (s, 1H), 7.33 (d, 1H, $J = 2.0$ Hz), 7.86 (d, 1H, $J = 8.4$ Hz), 12.37 (s, 1H); MS (ESI), m/z : 343.20 [M – H][–].

5.1.4.9. 4-(5-Methyl-4-phenylthiazol-2-ylamino)-4-oxobutanoic acid (**6j**). Yield 66.5%. ¹H NMR (DMSO-*d*₆, 400 MHz): δ 2.46 (s, 3H), 2.56 (t, 2H, $J = 6.4$ Hz), 2.66 (t, 2H, $J = 6.4$ Hz), 7.34 (d, 1H, $J = 7.6$ Hz), 7.45 (t, 2H, $J = 7.6$ Hz), 7.63 (d, 2H, $J = 7.6$ Hz), 12.13 (s, 1H), 12.22 (s, 1H); MS (ESI), m/z : 289.35 [M – H][–].

5.1.4.10. 4-((4-(4-Chlorophenyl)-5-methylthiazol-2-yl)amino)-4-oxobutanoic acid (**6k**). Yield 54.8%. ¹H NMR (DMSO-*d*₆, 400 MHz): δ 2.46 (s, 3H), 2.55 (t, 2H, $J = 6.4$ Hz), 2.65 (t, 2H, $J = 6.4$ Hz), 7.49 (d, 2H, $J = 8.8$ Hz), 7.65 (d, 2H, $J = 8.4$ Hz), 12.15 (s, 1H), 12.25 (s, 1H); ¹³C NMR (DMSO-*d*₆, 100 MHz): δ 12.28, 28.84, 30.27, 121.94, 128.86, 130.05, 132.25, 134.22, 143.15, 154.52, 170.79, 174.05; MS (ESI), m/z : 323.27 [M – H][–].

5.1.4.11. 4-((4-(Naphthalen-2-yl)thiazol-2-yl)amino)-4-oxobutanoic acid (**6l**). Yield 76.4%. ¹H NMR (DMSO-*d*₆, 400 MHz): δ 2.59 (t, 2H, $J = 6.4$ Hz), 2.71 (t, 2H, $J = 6.4$ Hz), 7.50–7.56 (m, 2H), 7.77 (s, 1H), 7.92–7.98 (m, 3H), 8.0 (d, 1H, $J = 8.4$ Hz), 12.26 (s, 1H), 12.39 (s, 1H); MS (ESI), m/z : 325.34 [M – H][–].

5.1.5. General procedure for the synthesis of 2-chloro-N-(4-(4-nitrophenyl)thiazol-2-yl)-acetamide

A mixture of 4-(4-nitrophenyl)thiazol-2-amine (1 g, 4.52 mmol) and Et₃N (1.28 mL, 6.72 mmol) in the DMF (30 mL) stirred below 10 °C, then followed by slow addition of 2-chloroacetyl chloride

(466 μ L, 5.88 mmol). After 4 h, the reaction quenched with water, filtered, and filtrate extracted with EtOAc. The combined organics were washed with water and dried (NaSO₄). The solution was evaporated to give compound **7b** as yellow solid (830 mg, 61.7% Yield). ¹H NMR (DMSO-*d*₆, 400 MHz): δ 4.44 (s, 2H), 8.07 (s, 1H), 8.16 (d, 2H, $J = 8.8$ Hz), 8.31 (d, 2H, $J = 9.2$ Hz), 12.78 (s, 1H); MS (ESI), m/z : 296.52 [M – H][–].

5.1.6. General procedure for the synthesis of 2-(2-(4-(4-nitrophenyl)thiazol-2-ylamino)-2-oxoethylthio)acetic acid

A mixture of 2-chloro-N-(4-(4-nitrophenyl)thiazol-2-yl)-acetamide (830 mg, 2.79 mmol), 2-mercaptoacetic acid (966.95 μ L, 13.95 mmol) and Et₃N (1.06 mL, 0.558 mmol) in anhydrous THF (42 mL) stirred at 35 °C overnight. The reaction quenched with water, filtered, and filtrate extracted with EtOAc. The combined organics were washed with water and dried (NaSO₄). The solution was evaporated to give compound **8b** as yellow solid (450 mg, 38.1% Yield). ¹H NMR (DMSO-*d*₆, 400 MHz): δ 3.44 (s, 2H), 3.66 (s, 2H), 8.03 (s, 1H), 8.15 (d, 2H, $J = 8.4$ Hz), 8.30 (d, 2H, $J = 8.4$ Hz), 12.54 (s, 1H), 12.72 (s, 1H); MS (ESI), m/z : 352.02 [M – H][–].

5.1.6.1. 2-(2-(4-(4-Chlorophenyl)thiazol-2-ylamino)-2-oxoethylthio)acetic acid (**8a**). Yield 45.8%. ¹H NMR (DMSO-*d*₆, 400 MHz): δ 3.56 (d, 2H, $J = 5.6$ Hz), 3.68 (s, 2H), 7.49 (d, 2H, $J = 8.8$ Hz), 7.72 (s, 1H), 7.90 (d, 2H, $J = 8.8$ Hz), 12.44 (s, 1H), 12.68 (s, 1H); ¹³C NMR (DMSO-*d*₆, 100 MHz): δ 34.25, 34.70, 109.45, 127.82, 129.23, 132.75, 133.54, 148.11, 158.39, 168.49, 171.36; MS (ESI), m/z : 341.82 [M – H][–].

5.1.6.2. 2-(2-(4-(4-Fluorophenyl)thiazol-2-ylamino)-2-oxoethylthio)acetic acid (**8c**). Yield 38.7%. ¹H NMR (DMSO-*d*₆, 400 MHz): δ 3.68 (s, 2H), 3.82 (s, 2H), 7.27 (t, 2H, $J = 8.8$ Hz), 7.64 (s, 1H), 7.91 (dd, $J_{1,2} = 5.2$ Hz, $J_{1,3} = 8.0$ Hz), 12.42 (s, 1H), 12.69 (s, 1H); MS (ESI), m/z : 325.10 [M – H][–].

5.1.6.3. 2-((2-Oxo-2-((4-(4-(trifluoromethyl)phenyl)thiazol-2-yl)amino)ethylthio)acetic acid (**8d**). Yield 32.4%. ¹H NMR (DMSO-*d*₆, 400 MHz): δ 3.44 (s, 2H), 3.56 (s, 2H), 7.79 (d, 2H, $J = 8.4$ Hz), 7.89 (s, 1H), 8.10 (d, 2H, $J = 8.0$ Hz), 12.49 (s, 1H), 12.68 (s, 1H); MS (ESI), m/z : 375.00 [M – H][–].

5.1.7. General procedure for the synthesis of 1-benzyl-1H-indole-3-carbaldehyde

A mixture of 1H-indole-3-carbaldehyde (1 g, 6.9 mmol) and KOH (570.86 mg, 10.2 mmol) in EtOH (66 mL) was stirred at room temperature when the solid was dissolved. The solvent was evaporated in vacuo, then added acetone (66 mL) and 1-(bromomethyl)-

2-fluorobenzene (1.22 mL, 10.2 mmol). The mixture was stirred at room temperature for 20 min, filtered, the filtrate was concentrated under reduced pressure. The residue was added a little water and put it in the refrigerator overnight. The precipitate was washed with water and vacuum dried to afford **11a** (636 mg, 39.2%). ¹H NMR (DMSO-*d*₆, 400 MHz): δ 5.36 (s, 2H), 7.17–7.20 (m, 2H), 7.29–7.37 (m, 5H), 7.71 (s, 1H), 8.32–8.34 (m, 1H), 10.00 (s, 1H); MS (ESI), *m/z*: 234.28 [M – H][–].

5.1.8. General procedure for the synthesis of (*E*)-3-(1-benzyl-1*H*-indol-3-yl)acrylic acid

A mixture of 1-benzyl-1*H*-indole-3-carbaldehyde (300 mg, 1.28 mmol) and malonic acid (332.28 mg, 3.19 mmol) in pyridine (9 mL) and piperidine (0.12 mL) was stirred at 100 °C for 12 h. After cooling to room temperature, the solution was added water (9 mL) and acidified with 6 N HCl while the precipitate produced. The reaction mixture was filtered, the solid was washed with water and EtOH. The product was recrystallised from acetone and PE as yellow solid. Yield 72.5%. ¹H NMR (DMSO-*d*₆, 400 MHz): δ 5.47 (s, 2H), 6.31 (d, 1H, *J* = 16.4 Hz), 7.19 (t, 2H, *J* = 7.2 Hz), 7.25 (t, 2H, *J* = 7.2 Hz), 7.28 (s, 1H), 7.33 (t, 2H, 7.2 Hz), 7.54 (d, 1H, *J* = 8.0 Hz), 7.78 (d, 1H, *J* = 16 Hz), 7.87 (d, 1H, *J* = 7.6 Hz), 8.12 (s, 1H), 11.95 (s, 1H); ¹³C NMR (DMSO-*d*₆, 100 MHz): δ 49.85, 111.64, 111.80, 113.26, 120.55, 121.67, 123.13, 126.22, 127.61, 128.07, 129.11, 134.61, 137.56, 137.79, 138.26, 169.00; MS (ESI), *m/z*: 276.41 [M – H][–].

5.1.8.1. (*E*)-3-(1-(2-Fluorobenzyl)-1*H*-indol-3-yl)acrylic acid (**12b**). Yield 66.7%. ¹H NMR (DMSO-*d*₆, 400 MHz): δ 5.53 (s, 2H), 6.31 (d, 1H, *J* = 16 Hz), 7.14–7.19 (m, 2H, *J*_{HH} = 7.6 Hz, *J*_{HF} = 8.0 Hz), 7.21–7.27 (m, 3H), 7.34–7.37 (m, 1H), 7.56 (d, 1H, *J* = 8.0 Hz), 7.77 (d, 1H, *J* = 16 Hz), 7.88 (d, 1H, *J* = 7.6 Hz), 8.05 (s, 1H), 11.97 (s, 1H); MS (ESI), *m/z*: 294.36 [M – H][–].

5.1.8.2. (*E*)-3-(1-(3-Fluorobenzyl)-1*H*-indol-3-yl)acrylic acid (**12c**). Yield 78.8%. ¹H NMR (DMSO-*d*₆, 400 MHz): δ 5.30 (s, 2H), 6.44 (d, 1H, *J* = 15.6 Hz), 6.82 (d, 1H, *J* = 9.2 Hz), 6.91 (d, 1H, 7.6 Hz), 6.98–7.01 (m, 1H), 7.28–7.32 (m, 4H, *J*_{HH} = 8.0 Hz, *J*_{HF} = 9.2 Hz), 7.46 (s, 1H), 7.95–7.98 (m, 1H), 8.01 (s, 1H); MS (ESI), *m/z*: 294.36 [M – H][–].

5.1.8.3. (*E*)-3-(1-(2-Methylbenzyl)-1*H*-indol-3-yl)acrylic acid (**12d**). Yield 80.5%. ¹H NMR (DMSO-*d*₆, 400 MHz): δ 2.36 (s, 3H), 5.47 (s, 3H), 6.32 (d, 1H, *J* = 16 Hz), 6.58 (d, 1H, *J* = 7.6 Hz), 7.07 (t, 1H, *J* = 7.2 Hz), 7.16–7.22 (m, 4H), 7.46–7.49 (m, 1H), 7.78 (d, 1H, *J* = 16 Hz), 7.9–7.92 (m, 2H), 11.96 (s, 1H); MS (ESI), *m/z*: 290.08 [M – H][–].

5.1.8.4. (*E*)-3-(1-(4-Methylbenzyl)-1*H*-indol-3-yl)acrylic acid (**12e**). Yield 60.0%. ¹H NMR (DMSO-*d*₆, 400 MHz): δ 2.24 (s, 3H), 5.40 (s, 2H), 6.29 (d, 1H, *J* = 16 Hz), 7.11–7.23 (m, 6H), 7.53 (d, 1H, *J* = 8.0 Hz), 7.77 (d, 1H, 16 Hz), 7.85 (d, 1H, *J* = 7.2 Hz), 8.09 (s, 1H), 11.96 (s, 1H); MS (ESI), *m/z*: 290.07 [M – H][–].

5.1.8.5. (*E*)-3-(1-(4-Isopropylbenzyl)-1*H*-indol-3-yl)acrylic acid (**12f**). Yield 65.8%. ¹H NMR (DMSO-*d*₆, 400 MHz): δ 1.14 (s, 3H), 1.15 (s, 3H), 2.83 (t, 1H, *J* = 6.8 Hz), 5.41 (s, 2H), 6.30 (d, 1H, *J* = 16 Hz), 7.17–7.25 (m, 6H), 7.57 (d, 1H, *J* = 7.6 Hz), 7.77 (d, 1H, *J* = 16 Hz), 7.86 (d, 1H, *J* = 7.6 Hz), 8.10 (s, 1H), 11.94 (s, 1H); MS (ESI), *m/z*: 318.03 [M – H][–].

5.1.8.6. (*E*)-3-(1-(4-(*tert*-Butyl)benzyl)-1*H*-indol-3-yl)acrylic acid (**12g**). Yield 77.6%. ¹H NMR (DMSO-*d*₆, 400 MHz): δ 1.22 (s, 9H), 5.41 (s, 2H), 6.30 (d, 1H, *J* = 16 Hz), 7.17–7.25 (m, 4H), 7.32 (d, 1H, 8.0 Hz), 7.75 (d, 1H, *J* = 16 Hz), 7.86 (d, 1H, *J* = 7.6 Hz), 8.10 (s, 1H), 11.94 (s, 1H); ¹³C NMR (DMSO-*d*₆, 100 MHz): δ 31.49, 34.64, 49.49, 111.65, 111.76, 113.20, 120.52, 121.62, 123.10, 125.84, 126.20, 127.41, 134.54, 137.56, 138.26, 150.47, 168.99; MS (ESI), *m/z*: 332.07 [M – H][–].

5.1.8.7. (*E*)-3-(1-(4-Nitrobenzyl)-1*H*-indol-3-yl)acrylic acid (**12h**). Yield 45.6%. ¹H NMR (DMSO-*d*₆, 400 MHz): δ 5.65 (s, 2H), 6.34 (d, 1H, *J* = 16 Hz), 7.19–7.24 (m, 2H), 7.44 (d, 2H, *J* = 8.4 Hz), 7.49 (dd, 1H, *J*_{1,2} = 2.8 Hz, *J*_{1,3} = 7.2 Hz), 7.77 (d, 1H, *J* = 16 Hz), 7.89 (dd, 1H, *J*_{1,2} = 2.0 Hz, *J*_{1,3} = 5.6 Hz), 8.12 (s, 1H), 8.18 (d, 1H, *J* = 8.8 Hz), 12.05 (s, 1H); MS (ESI), *m/z*: 321.27 [M – H][–].

5.1.8.8. (*E*)-3-(1-(4-Cyanobenzyl)-1*H*-indol-3-yl)acrylic acid (**12i**). Yield 58.0%. ¹H NMR (DMSO-*d*₆, 400 MHz): δ 5.60 (s, 2H), 6.33 (d, 1H, *J* = 16 Hz), 7.19–7.25 (m, 2H), 7.37 (d, 2H, *J* = 8.0 Hz), 7.50 (d, 1H, *J* = 8.4 Hz), 7.80 (t, 3H, *J* = 8.0 Hz), 7.89 (d, 1H, *J* = 8.0 Hz), 8.12 (s, 1H), 11.98 (s, 1H); MS (ESI), *m/z*: 301.34 [M – H][–].

5.1.8.9. (*E*)-3-(1-(3-Fluorobenzyl)-2-methyl-1*H*-indol-3-yl)acrylic acid (**12j**). Yield 78.2%. ¹H NMR (DMSO-*d*₆, 400 MHz): δ 5.98 (s, 2H), 6.31 (d, 1H, *J* = 16 Hz), 6.88 (d, 1H, *J* = 6.8 Hz), 7.20–7.25 (m, 2H), 7.41 (t, 1H, *J* = 8.0 Hz), 7.55–7.63 (m, 3H), 7.77 (d, 1H, *J* = 16 Hz), 7.88–7.93 (m, 2H), 7.98 (d, 1H, *J* = 1.6 Hz), 8.00 (s, 1H), 8.16 (d, 1H, *J* = 8.4 Hz), 11.94 (s, 1H); MS (ESI), *m/z*: 326.00 [M – H][–].

5.1.8.10. (*E*)-3-(1-(4-Fluorobenzyl)-1*H*-indol-3-yl)acrylic acid (**12k**). Yield 68.4%. ¹H NMR (DMSO-*d*₆, 400 MHz): δ 5.40 (s, 2H), 6.25 (d, 1H, *J* = 16.0 Hz), 6.83 (dd, 1H, *J*_{1,2} = 2.4 Hz, *J*_{1,3} = 8.8 Hz), 7.15 (t, 2H, *J* = 8.8 Hz), 7.28–7.31 (m, 3H, *J*_{HH} = 6.0 Hz, *J*_{HF} = 7.6 Hz), 7.43 (d, 1H, *J* = 8.8 Hz), 7.76 (d, 1H, *J* = 16.0 Hz), 8.06 (s, 1H); MS (ESI), *m/z*: 294.36 [M – H][–].

5.1.9. General procedure for the synthesis of 5-methyl-1*H*-indole-3-carbaldehyde

To a 100 mL three-necked round flask was introduced anhydrous *N,N*-dimethylformamide (4.2 mL, 34.35 mmol) at 0 °C under argon followed by slow addition of phosphorus oxychloride (1.3 mL, 13.62 mmol). Solution was mixed at 0 °C for 40 min. A solution of 5-methyl-1*H*-indole (1.627 g, 12.41 mmol) in 2.5 mL of DMF was slowly added maintaining the temperature below 10 °C. The solution was stirred for 40 min at 0 °C and then 35 °C for additional 40 min. Then ice was added to the flask and a solution of sodium hydroxide (5.5 g, 137.25 mmol dissolved in 14.6 mL of water) was introduced using a dropping funnel. Solution was vigorously stirred during the addition, then heated to 100 °C for 30 min and left to reach room temperature. The brown precipitate was filtered off and washed with large volumes of water. The powder was dried in vacuum. Yield 71.5%. ¹H NMR (DMSO-*d*₆, 400 MHz): δ 2.41 (s, 3H), 7.07 (d, 1H, *J* = 8.4 Hz), 7.38 (d, 1H, *J* = 8.0 Hz), 7.90 (s, 1H), 8.32 (s, 1H), 9.89 (s, 1H), 12.01 (s, 1H); MS (ESI), *m/z*: 158.10 [M – H][–].

5.1.10. General procedure for the synthesis of 1-(2-fluorobenzyl)-5-methyl-1*H*-indole-3-carbaldehyde

A mixture of 5-methyl-1*H*-indole-3-carbaldehyde (500 mg, 3.14 mmol) and KOH (263.85 mg, 4.71 mmol) in EtOH (35 mL) was stirred at room temperature when the solid was dissolved. The solvent was evaporated in vacuo, then added acetone (35 mL) and 1-(bromo-methyl)-2-fluorobenzene (568 μL, 4.71 mmol). The mixture was stirred at room temperature for 20 min, filtered, the filtrate was concentrated under reduced pressure. The residue was added a little water and put it in the refrigerator overnight. The precipitate was washed with water and vacuum dried to afford **15a** (580 mg, 69.0% Yield). ¹H NMR (DMSO-*d*₆, 400 MHz): δ 2.40 (s, 3H), 5.57 (s, 2H), 7.10–7.18 (m, 2H), 7.20–7.27 (m, 2H), 7.36 (d, 1H, *J* = 7.2 Hz), 7.46 (d, 1H, *J* = 8.0 Hz), 7.93 (s, 1H), 8.34 (s, 1H), 9.91 (s, 1H); MS (ESI), *m/z*: 266.20 [M – H][–].

5.1.11. General procedure for the synthesis of (*E*)-3-(1-(2-fluorobenzyl)-5-methyl-1*H*-indol-3-yl)acrylic acid

A mixture of 1-(2-fluorobenzyl)-5-methyl-1*H*-indole-3-carbaldehyde (580 mg, 2.17 mmol) and malonic acid (565 mg,

5.42 mmol) in pyridine (16 mL) and piperidine (0.25 mL) was stirred at 100 °C for 12 h. After cooling to room temperature, the solution was added water (16 mL) and acidified with 6 N HCl while the precipitate produced. The reaction mixture was filtered, the solid was washed with water and EtOH. The product was recrystallised from acetone and PE as yellow solid. Yield 44.6%. ¹H NMR (DMSO-*d*₆, 400 MHz): δ 2.42 (s, 3H), 5.48 (s, 2H), 6.29 (d, 1H, *J* = 16.0 Hz), 7.06 (d, 1H, *J* = 8.4 Hz), 7.09–7.16 (m, 2H, *J*_{HH} = 6.0 Hz, *J*_{HF} = 7.6 Hz), 7.23 (t, 1H, *J* = 9.2 Hz), 7.34 (t, 1H, *J* = 6.8 Hz), 7.42 (d, 1H, *J* = 8.8 Hz), 7.68 (s, 1H), 7.74 (d, 1H, *J* = 16.0 Hz), 7.97 (s, 1H), 12.01 (s, 1H); ¹³C NMR (DMSO-*d*₆, 100 MHz): δ 21.59, 43.99, 111.05, 111.55, 113.09, 115.88, 120.38, 124.53, 125.15, 125.18, 126.33, 130.00, 134.69, 135.97, 138.29, 148.79, 159.20, 161.64, 169.02; MS (ESI), *m/z*: 308.00 [M – H][–].

5.1.11.1. (*E*)-3-(1-(2-Fluorobenzyl)-5-methoxy-1H-indol-3-yl)acrylic acid (**16b**). Yield 56.2%. ¹H NMR (DMSO-*d*₆, 400 MHz): δ (d, 3H, *J* = 9.6 Hz), 5.48 (s, 2H), 6.25 (d, 1H, *J* = 16.0 Hz), 6.86 (dd, 1H, *J*_{1,2} = 2.0 Hz, *J*_{1,3} = 9.2 Hz), 7.11–7.16 (m, 2H, *J*_{HH} = 7.6 Hz, *J*_{HF} = 7.6 Hz), 7.23 (t, 1H, *J* = 9.2 Hz), 7.29 (d, 1H, *J* = 2.4 Hz), 7.32–7.36 (m, 1H), 7.44 (d, 1H, *J* = 8.8 Hz), 7.76 (d, 1H, *J* = 16.0 Hz), 8.00 (s, 1H), 11.91 (s, 1H); MS (ESI), *m/z*: 324.00 [M – H][–].

5.1.11.2. (*E*)-3-(1-(2-Fluorobenzyl)-2-methyl-1H-indol-3-yl)acrylic acid (**16c**). Yield 74.9%. ¹H NMR (CDCl₃, 400 MHz): δ 2.51 (s, 3H), 5.35 (s, 2H), 6.48 (d, 1H, *J* = 16.0 Hz), 6.68 (d, 1H, *J* = 9.2 Hz), 6.75 (d, 1H, *J* = 8.0 Hz), 6.93–6.98 (m, 1H), 7.24–7.30 (m, 4H, *J*_{HH} = 8.0 Hz, *J*_{HF} = 8.4 Hz), 7.96 (d, 1H, *J* = 7.6 Hz), 8.09 (d, 1H, *J* = 16.0 Hz), 12.01 (s, 1H); ¹³C NMR (DMSO-*d*₆, 100 MHz): δ 10.81, 46.05, 108.94, 110.92, 112.67, 113.50, 114.55, 120.11, 121.94, 122.62, 124.36, 125.72, 131.26, 137.47, 140.81, 142.66, 150.05, 161.57, 164.60, 169.16; MS (ESI), *m/z*: 308.04 [M – H][–].

5.1.11.3. (*E*)-3-(1-(3-Fluorobenzyl)-5-methyl-1H-indol-3-yl)acrylic acid (**16d**). Yield 68.3%. ¹H NMR (DMSO-*d*₆, 400 MHz): δ 2.42 (s, 3H), 5.45 (s, 2H), 6.30 (d, 1H, *J* = 16.0 Hz), 7.03–7.12 (m, 4H, *J*_{HH} = 6.8 Hz, *J*_{HF} = 7.2 Hz), 7.33 (q, 1H, *J*_{1,2} = 7.6 Hz, *J*_{1,3} = 14.0 Hz), 7.42 (d, 1H, *J* = 8.4 Hz), 7.68 (s, 1H), 7.75 (d, 1H, *J* = 16.0 Hz), 8.05 (s, 1H), 11.96 (s, 1H); MS (ESI), *m/z*: 308.04 [M – H][–].

5.1.11.4. (*E*)-3-(1-(3-Fluorobenzyl)-5-methoxy-1H-indol-3-yl)acrylic acid (**16e**). Yield 76.7%. ¹H NMR (DMSO-*d*₆, 400 MHz): δ 3.79 (s, 3H), 5.44 (s, 2H), 6.25 (d, 1H, *J* = 16.0 Hz), 6.84 (dd, 1H, *J*_{1,2} = 2.4 Hz, *J*_{1,3} = 8.8 Hz), 7.03–7.12 (m, 3H, *J*_{HH} = 8.0 Hz, *J*_{HF} = 8.0 Hz), 7.29 (d, 1H, *J* = 2.0 Hz), 7.33 (q, 1H, *J*_{1,2} = 7.6 Hz, *J*_{1,3} = 14.0 Hz), 7.43 (d, 1H, *J* = 8.8 Hz), 7.77 (d, 1H, *J* = 16.0 Hz), 8.08 (s, 1H), 11.91 (s, 1H); MS (ESI), *m/z*: 324.00 [M – H][–].

5.1.11.5. (*E*)-3-(1-(4-Fluorobenzyl)-5-methoxy-1H-indol-3-yl)acrylic acid (**16f**). Yield 66.4%. ¹H NMR (DMSO-*d*₆, 400 MHz): δ 3.79 (s, 3H), 5.40 (s, 2H), 6.25 (d, 1H, *J* = 16.0 Hz), 6.83 (dd, 1H, *J*_{1,2} = 2.4 Hz, *J*_{1,3} = 8.8 Hz), 7.15 (t, 2H, *J* = 8.8 Hz), 7.28–7.31 (m, 3H, *J*_{HH} = 6.0 Hz, *J*_{HF} = 7.6 Hz), 7.43 (d, 1H, *J* = 8.8 Hz), 7.76 (d, 1H, *J* = 16.0 Hz), 8.06 (s, 1H); MS (ESI), *m/z*: 324.00 [M – H][–].

5.1.11.6. (*E*)-3-(1-(3-Fluorobenzyl)-2-methyl-1H-indol-3-yl)acrylic acid (**16g**). Yield 65.3%. ¹H NMR (CDCl₃, 400 MHz): δ 2.53 (s, 3H), 5.41 (s, 2H), 6.48 (d, 1H, *J* = 16.0 Hz), 6.51 (d, 1H, *J* = 14.4 Hz), 6.97 (t, 1H, *J* = 7.6 Hz), 7.12 (t, 1H, *J* = 8.8 Hz), 7.22–7.29 (m, 3H, *J*_{HH} = 7.2 Hz, *J*_{HF} = 8.0 Hz), 7.96 (m, 2H), 8.09 (d, 1H, *J* = 16.0 Hz), 8.86 (d, 1H, *J* = 4.8 Hz); MS (ESI), *m/z*: 308.05 [M – H][–].

5.1.12. General procedure for the synthesis of 2-(1-benzyl-1H-indol-3-yl)acetic acid

A mixture of 2-(1H-indol-3-yl)acetic acid (2 g, 11.4 mmol) and NaH (1.1 g, 45.8 mmol) in anhydrous DMF (20 mL) stirred at 0 °C

for 30 min. The solution was stirred at 0 °C followed by slow addition of 1-(bromomethyl)benzene (1.80 mL, 13.7 mmol) for another 1 h. After the reaction was completed, put the mixture into water (150 mL) and acidified with 4 N HCl while the precipitate produced. The white precipitate was filtered off, washed with water and EtOH, vacuum dried to afford **18a** (2.49 g, 82.3% Yield). ¹H NMR (CDCl₃, 400 MHz): δ 3.66 (s, 2H), 5.38 (s, 2H), 7.01 (t, 1H, *J* = 7.2 Hz), 7.10 (t, 1H, *J* = 7.6 Hz), 7.19 (d, 2H, *J* = 7.6 Hz), 7.23 (d, 1H, *J* = 7.2 Hz), 7.30 (t, 2H, *J* = 7.2 Hz), 7.41 (t, 2H, *J* = 8.8 Hz), 7.50 (d, 1H, *J* = 7.6 Hz), 12.22 (s, 1H); ¹³C NMR (DMSO-*d*₆, 100 MHz): δ 31.32, 49.38, 108.14, 110.51, 119.22, 119.45, 121.78, 127.56, 127.79, 128.12, 128.99, 136.39, 138.78, 173.52; MS (ESI), *m/z*: 264.31 [M – H][–].

5.1.12.1. 2-(1-(2-Methyl-1H-indol-3-yl)acetic acid (**18b**). Yield 85.2%. ¹H NMR (DMSO-*d*₆, 400 MHz): δ 2.30 (s, 3H), 3.66 (s, 2H), 5.37 (s, 2H), 6.57 (d, 1H, *J* = 7.6 Hz), 7.01–7.10 (m, 3H), 7.11–7.19 (m, 2H), 7.21 (s, 1H), 7.35 (d, 1H, *J* = 8.4 Hz), 7.53 (d, 1H, *J* = 7.6 Hz), 12.28 (s, 1H); MS (ESI), *m/z*: 278.45 [M – H][–].

5.1.12.2. 2-(1-(2-Fluorobenzyl)-1H-indol-3-yl)acetic acid (**18c**). ¹H NMR (DMSO-*d*₆, 400 MHz): δ 3.65 (s, 2H), 5.44 (s, 2H), 7.03 (t, 1H, *J* = 7.6 Hz), 7.07–7.14 (m, 3H, *J*_{HH} = 7.6 Hz, *J*_{HF} = 9.2 Hz), 7.22 (t, 1H, *J* = 9.2 Hz), 7.30–7.34 (m, 1H), 7.35 (s, 1H), 7.44 (d, 1H, *J* = 8.4 Hz), 7.51 (d, 1H, *J* = 7.6 Hz), 12.23 (s, 1H); MS (ESI), *m/z*: 282.30 [M – H][–].

5.1.12.3. 2-(1-(3-Fluorobenzyl)-1H-indol-3-yl)acetic acid (**18d**). Yield 88.6%. ¹H NMR (DMSO-*d*₆, 400 MHz): δ 3.67 (s, 2H), 5.41 (s, 2H), 7.00–7.05 (m, 3H, *J*_{HH} = 7.6 Hz, *J*_{HF} = 7.2 Hz), 7.07 (d, 1H, *J* = 1.6 Hz), 7.11 (t, 1H, *J* = 7.2 Hz), 7.32 (q, 1H, *J*_{1,2} = 8.0 Hz, *J*_{1,3} = 14.4 Hz), 7.42 (s, 1H), 7.44 (s, 1H), 7.51 (d, 1H, *J* = 8.0 Hz), 12.25 (s, 1H); MS (ESI), *m/z*: 282.30 [M – H][–].

5.1.12.4. 2-(1-(4-Fluorobenzyl)-1H-indol-3-yl)acetic acid (**18e**). Yield 80.5%. ¹H NMR (DMSO-*d*₆, 400 MHz): δ 3.65 (s, 2H), 5.37 (s, 2H), 7.01 (t, 1H, *J* = 7.2 Hz), 7.08 (d, 1H, *J* = 1.6 Hz), 7.10–7.16 (m, 2H, *J*_{HH} = 8.8 Hz, *J*_{HF} = 9.2 Hz), 7.24–7.28 (m, 2H), 7.40 (s, 1H), 7.43 (d, 1H, *J* = 8.4 Hz), 7.50 (d, 1H, *J* = 7.6 Hz), 12.23 (s, 1H); MS (ESI), *m/z*: 282.30 [M – H][–].

5.2. Biological methods

5.2.1. TNF-α inhibition assay

RAW 264.7 cells were seeded in wells and incubated for 24 h. After incubation, the cells were incubated with all compounds of different concentrations in the presence of LPS (1 μg/mL) for 24 h. The TNF-α concentration in the culture medium was determined by ELISA kit (R&D Systems, Minneapolis, MN).

5.2.2. Apparent K_i values

1,8-ANS was dissolved in absolute ethanol and diluted with 25 mM Tris–HCl (pH 7.4) to a final concentration of 5 μM (final EtOH concentration of 0.05%). Rat ap2 protein was titrated into 500 μL 1,8-ANS and the fluorescence enhancement was measured using a Perkin–Elmer 650-10S fluorescence spectrophotometer with 4 nm excitation and emission slit widths. **12b** (diluted from a 10 mM stock in absolute ethanol) was added to the ap2/1,8-ANS complex, mixed for 45 s, and the fluorescence signal was recorded. The decay in corrected fluorescence intensity as a function of competitor concentration was used to determine the midpoint of the competition (*I*₅₀).

An apparent K_i value was calculated using $K_i = [I_{50}]/(1 + [L]/K_d)$, where [L] = free concentration of 1,8-ANS, and K_d = apparent dissociation constant of ap2 for 1,8-ANS.

5.2.3. Animals

Male C57BL/6J mice (age range: 7–8 weeks) were purchased from Western China Experimental Animal Center. The animals were fed a normal diet or a high-fat diet (kcal: 60% of energy derived from fat, 20% from protein and 20% from carbohydrates, D12494 Research Diet, USA) throughout the study, which was used to establish the HF of diet-induced obesity (DIO). After 8 weeks, the DIO mice were divided into two groups (control and **12b**-treated; $n = 8$ per group). The **12b**-treated groups were administered with **12b** orally everyday at a dose of 50 mg/kg. The compound **12b** suspended in Tween 80 and 5% saline (Sigma–Aldrich, St. Louis, MO). Body weight was recorded during the study period. After the experimental period, animals were sacrificed, photographed for morphology of abdomen adipose, while their inguinal white adipose tissue (WAT), muscle and whole body tissue composition was extracted for evaluation of other parameters.

5.2.3.1. Oral glucose tolerance test. Mice were fasted for 12 h before the OGTT. At 0 min, a drop of blood was taken via a tail nick before giving the oral glucose load. Mice were then given 5% glucose (0.5 g/kg). Blood samples were obtained at 15, 30, 60, 90 and 120 min following glucose ingestion. The blood glucose was determined by a glucose meter.

5.2.3.2. Insulin tolerance test. Mice were fasted for 12 h and then given an intraperitoneal injection of insulin (2 U/Kg) in saline. Blood samples were taken at 0, 15, 30, 60, 90 and 120 min for the determination of blood glucose with a glucose meter.

5.2.3.3. Plasma measurements. After 8 weeks treatment, blood was collected from the heart under anaesthesia. Samples were centrifuged at 5,000 g for 15 min at 4 °C. Plasma was analyzed for total cholesterol (TC), triglycerides (TG), alanine transaminase (ALT) and glucose, which were measured with a multifunctional biochemistry analyzer Olympus AU2700 (Olympus, Tokyo, Japan).

5.2.3.4. Histopathological examination. Liver samples were fixed in 4% buffered formalin and embedded in Tissue-Tek OCT compound and paraffin for histological analysis. Formalin-fixed and paraffin-embedded section was processed routinely for H&E staining. The OCT-embedded samples were serially sectioned at 4 μm.

Acknowledgments

This study was supported by National Key Technologies R&D Program (grant number: 2012ZX09103-101-033).

References

[1] F. Masakazu, H. Tetsuya, I. Naoko, Design, synthesis and bioactivities of novel diarylthiophenes: inhibitors of tumor necrosis factor- α (TNF- α) production, *Bioorg. Med. Chem.* 10 (2002) 3113–3122.

[2] P.C. William, K.S. Jaswinder, TNF- α and adipocyte biology, *FEBS Lett.* 582 (2008) 117–131.

[3] G.S. Hotamisligil, Mechanisms of TNF- α -induced insulin resistance, *Exp. Clin. Endocrinol. Diabetes* 107 (1999) 119–125.

[4] H. Xu, J. Hirosumi, K.T. Uysal, A.D. Guler, G.S. Hotamisligil, Exclusive action of transmembrane TNF- α in adipose tissue leads to reduced adipose mass and local but not systemic insulin resistance, *Endocrinology* 143 (2002) 1502–1511.

[5] K.T. Uysal, S.M. Wiesbrock, M.W. Marino, G.S. Hotamisligil, Protection from obesity-induced insulin resistance in mice lacking TNF- α function, *Nature* 389 (1997) 610–614.

[6] K.T. Uysal, S.M. Wiesbrock, G.S. Hotamisligil, Functional analysis of tumor necrosis factor (TNF) receptors in TNF- α -mediated insulin resistance in genetic obesity, *Endocrinology* 139 (1998) 4832–4838.

[7] L. Scheja, L. Makowski, K.T. Uysal, S.M. Wiesbrock, D.R. Shimshek, D.S. Meyers, M. Morgan, R.A. Parker, G.S. Hotamisligil, Altered insulin secretion associated with reduced lipolytic efficiency in *ap2* $-/-$ mice, *Diabetes* 48 (1999) 1987–1994.

[8] L. Makowski, K.C. Brittingham, J.M. Reynolds, J. Suttles, G.S. Hotamisligil, The fatty acid-binding protein, *ap2*, coordinates macrophage cholesterol trafficking and inflammatory activity, *J. Biol. Chem.* 280 (2005) 12888–12895.

[9] G.S. Hotamisligil, R.S. Johnson, R.J. Distel, R. Ellis, V.E. Papaioannou, B.M. Spiegelman, Uncoupling of obesity from insulin resistance through a targeted mutation in *ap2*, the adipocyte fatty acid binding protein, *Science* 274 (1996) 1377–1379.

[10] M. Furuhashi, G. Tuncman, C.Z. Görgün, L. Makowski, G. Atsumi, E. Vaillancourt, K. Kono, V.R. Babaev, S. Fazio, M.F. Linton, R. Sulsky, J.A. Robl, R.A. Parker, G.S. Hotamisligil, Treatment of diabetes and atherosclerosis by inhibiting fatty-acid-binding protein *ap2*, *Nature* 447 (2007) 959–965.

[11] A.V. Hertz, K. Hellberg, J.M. Reynolds, A.C. Kruse, B.E. Juhlmann, A.J. Smith, M.A. Sanders, D.H. Ohlendorf, J. Suttles, D.A. Bernlohr, Identification and characterization of a small molecule inhibitor of fatty acid binding proteins, *J. Med. Chem.* 52 (2009) 6024–6031.

[12] L. Fredrik, H. Saba, A. Eva, M. Carmen, U. Jonas, S. Stefan, L. Thomas, R. Lena, B. Tjeerd, Discovery of inhibitors of human adipocyte fatty acid-binding protein, a potential type 2 diabetes target, *Bioorg. Med. Chem. Lett.* 14 (2004) 4445–4448.

[13] D. Alexandra, B. Anne, E. Johan, D. Muriel, L.B. Guillaume, G. Nicole, P. Jean-Yves, New *N*-pyridinyl(methyl)-indolalkanamides acting as topical inflammation inhibitors, *Bioorg. Med. Chem. Lett.* 14 (2004) 5441–5444.

[14] A. Andreani, M. Rambaldi, A. Locatelli, G. Pifferi, Synthesis and anti-inflammatory activity of indolylacrylic and methylacrylic acids, *Eur. J. Med. Chem.* 29 (1994) 903–906.

[15] S. PengAn, W. Binli, Synthesis of *p* methoxy bromoacetophenone by substituting cupric bromide for liquid bromine, *Liaoning Chem. Ind.* 32 (2003) 17–18.

[16] A. Andreani, M. Rambaldi, A. Locatelli, F. Andreani, R. Bossa, I. Galatulas, M. Ninci, Synthesis and analgesic activity of 1-(*N*-methylanilinoethyl)indoles, *Eur. J. Med. Chem.* 3 (1991) 125–129.

[17] G. Francis, L. Cedric, P. Fabrice, C. Damien, B. Sophie, P. Carine, L.P. Patrice, L.B. Marc, Design, synthesis and evaluation of 3-(imidazol-1-ylmethyl)indoles as antileishmanial agents, *J. Enzym. Inhib. Med. Chem.* 24 (2009) 1067–1075.

[18] H.M. Berman, J. Westbrook, Z. Feng, G. Gilliland, T.N. Bhat, H. Weissig, I.N. Shindyalov, P.E. Bourne, The protein data bank, *Nucleic Acids Res.* 28 (2000) 235–242.

[19] R.E. Gillilan, S.D. Ayers, N. Noy, Structural basis for activation of fatty acid-binding protein 4, *J. Mol. Biol.* 372 (2007) 1246–1260.

[20] A. Jakalian, B.L. Bush, D.B. Jack, C.I. Bayly, Fast, efficient generation of high-quality atomic charges. AM1-BCC HF: I. Method, *J. Comput. Chem.* 21 (2000) 132–146.

[21] A. Jakalian, D.B. Jack, C.I. Bayly, Fast, efficient generation of high-quality atomic charges. AM1-BCC HF: II. Parameterization and validation, *J. Comput. Chem.* 23 (2002) 1623–1641.

[22] T.A. Halgren, Merck molecular force field. I. Basis, form, scope, parameterization, and performance of MMFF94, *J. Comput. Chem.* 17 (1996) 490–519.